Check for updates

**ARTICLE**

# Comprehensive genomic profiling of *EWSR1/FUS::CREB* translocation-associated tumors uncovers prognostically significant recurrent genetic alterations and methylation-transcriptional correlates

Josephine K. Dermawan [ID][1], Fabio Vanoli[1], Laurie Herviou[1], Yun-Shao Sung[1], Lei Zhang[1], Samuel Singer[2], William D. Tap[3], Ryma Benayed[1], Tejus A. Bale [ID][1], Jamal K. Benhamida [ID][1], Brendan C. Dickson [ID][4] and Cristina R. Antonescu [ID][1✉]

To elucidate the mechanisms underlying the divergent clinicopathologic spectrum of *EWSR1/FUS::CREB* translocation-associated tumors, we performed a comprehensive genomic analysis of fusion transcript variants, recurrent genetic alterations (mutations, copy number alterations), gene expression, and methylation profiles across a large cohort of tumor types. The distribution of the *EWSR1/FUS* fusion partners—*ATF1*, *CREB1*, and *CREM*—and exon involvement was significantly different across different tumor types. Our targeted sequencing showed that secondary genetic events are associated with tumor type rather than fusion type. Of the 39 cases that underwent targeted NGS testing, 18 (46%) had secondary OncoKB mutations or copy number alterations (29 secondary genetic events in total), of which 15 (52%) were recurrent. Secondary recurrent, but mutually exclusive, *TERT* promoter and *CDKN2A* mutations were identified only in clear cell sarcoma (CCS) and associated with worse overall survival. *CDKN2A/B* homozygous deletions were recurrent in angiomatoid fibrous histiocytoma (AFH) and restricted to metastatic cases. mRNA upregulation of *MITF*, *CDH19*, *PARVB*, and *PFKP* was found in CCS, compared to AFH, and correlated with a hypomethylated profile. In contrast, *S100A4* and *XAF1* were differentially upregulated and hypomethylated in AFH but not CCS. Unsupervised clustering of methylation profiles revealed that CREB family translocation-associated tumors form neighboring but tight, distinct clusters. A sarcoma methylation classifier was able to accurately match 100% of CCS cases to the correct methylation class; however, it was suboptimal when applied to other histologies. In conclusion, our comprehensive genomic profiling of *EWSR1/FUS:: CREB* translocation-associated tumors uncovered mostly histotype, rather than fusion-type associated correlations in transcript variants, prognostically significant secondary genetic alterations, and gene expression and methylation patterns.

## INTRODUCTION

Recurrent gene fusions involving *EWSR1/FUS* with members of the cAMP response element binding protein (CREB) family (*ATF1*, *CREB1* and *CREM*) are shared amongst multiple tumor-types spanning a wide clinicopathologic spectrum. Despite sharing related gene fusions, members of the *EWSR1::CREB* family of translocation-associated tumors exhibit significantly different clinicopathologic characteristics. The prototypic example is angiomatoid fibrous histiocytoma (AFH) vs clear cell sarcoma (CCS)—two morphologically distinct tumors, the former mostly associated with a benign behavior, while the latter being an aggressive sarcoma with a high metastatic potential and poor outcome, as illustrated by the survival analysis of our cohort. Clear cell sarcoma-like tumor of gastrointestinal tract (GICCS, also known as gastrointestinal neuroectodermal tumor) and hyalinizing clear cell carcinoma of salivary gland (HCCC) had intermediate overall survival relative to AFH and CCS.

To elucidate the molecular mechanisms underlying their differences, we performed a comprehensive genomic analysis of fusion transcript variants, secondary recurrent genetic alterations (mutations, copy number alterations), gene expression and methylation profiles across a large cohort of tumour-types defined by *EWSR1/FUS::CREB* gene fusions. Specifically, the tumors included in this study encompassed AFH, CCS, GICCS, HCCC, clear cell odontogenic carcinoma (CCOC), malignant epithelioid neoplasm with predilection for mesothelial-lined cavities (ME), mesothelioma (Meso), myxoid mesenchymal tumor (MMT), and primary pulmonary myxoid sarcoma (PPMS).

[1]Department of Pathology, Memorial Sloan Kettering Cancer Center, New York, NY, USA. [2]Department of Surgery, Memorial Sloan Kettering Cancer Center, New York, NY, USA. [3]Department of Medicine, Sarcoma Service, Memorial Sloan Kettering Cancer Center, New York, NY, USA. [4]Department of Pathology and Laboratory Medicine, Sinai Health System, Toronto, ON, Canada. ✉email: antonesc@mskcc.org

## MATERIALS AND METHODS

### Case selection and study cohort

After approval from the Institutional Review Board, cases were identified from the Memorial Sloan Kettering Cancer Center (MSKCC) surgical pathology archives, or from collaborating institutions, based on tumor types and/or presence of *EWSR1/FUS::ATF1/CREB1/CREM* fusions. The diagnosis of all 137 cases included molecular confirmation of both fusion partners: 37 cases by fluorescence in situ hybridization, 24 cases by reverse transcription PCR (RT-PCR), 29 cases by Memorial Sloan Kettering-Integrated Mutation Profiling of Actionable Cancer Targets (MSK-IMPACT) only, 10 cases by MSK-Fusion only, 10 cases by both MSK-IMPACT and MSK-Fusion, 21 cases by TruSight RNA Fusion Panel (Illumina, San Diego, CA), with the remaining cases based on NGS testing performed by referring institutions. The meta-analysis of the published literature was based on an exhaustive literature search on any fusions or gene rearrangements reported in all of the listed entities in Supplementary Table 1 that we could identify on PubMed.

### DNA seq and RNA seq

Detailed descriptions of MSK-IMPACT workflow and data analysis, a hybridization capture-based targeted DNA NGS assay for solid tumor, and MSK-Fusion, an amplicon-based targeted RNA NGS assay using the Archer™ FusionPlex™ standard protocol, were described previously[1,2].

### 850k methylation array

Details of the methylation array protocol were described previously[3]. Briefly, for each sample, 250 ng of input DNA was used for bisulfite conversion (EZ DNA Methylation Kit; Zymo Research; catalog number D5002), followed by an FFPE restoration step using the Infinium HD FFPE DNA Restore Kit (Illumina; catalog number WG-321-1002). All samples were processed on the Infinium methylationEPIC 850k BeadChip array and scanned using the Illumina iScan. Each CpG site interrogated by the Infinium array was identified by a unique cg identifier in the format of cg#, where # is a number. The methylation level for each CpG site was quantified using β values (continuous values between zero and one), calculated as the ratio of methylated signal/total signal plus an offset. 850k methylation array profiling was performed in a total of 80 samples, including: 7 AFH, 4 CCS, 8 GICCS, and compared to 51 soft tissue tumors of various histotypes (4 angiosarcomas, 27 gastrointestinal stromal tumors, 1 HCCC, 1 ME, 3 Meso, 11 paragangliomas, 4 small blue round cell tumors) and 10 normal tissues (8 human peripheral white blood cell samples, 2 normal adrenal medulla). A minimum cutoff of $\log_2FC$ (fold change) >1.0 and FDR < 0.01 was used for statistical analysis of differential methylation analysis using $t$ test, focusing on comparison of the 7 AFH against all other samples and 4 CCS against all other samples. Unsupervised hierarchical clustering was performed by the t-distributed stochastic neighborhood embedding (t-SNE) method using aforementioned samples and additional raw IDAT files downloaded from the Heidelberg sarcoma methylation classifier reference cohort[4] (see supplementary figure 3 for sample and method details).

### Sarcoma classification by DNA methylation profiling

Details of the DNA methylation-based machine learning sarcoma classification algorithm were described in Koelsche et al[4]. This random forest-based machine learning algorithm was developed at the German Cancer Research Center (DKFZ) in Heidelberg, Germany. Briefly, the method defines 62 methylation classes based on a reference cohort of 1077 samples encompassing a broad range of sarcomas. The classifier quantifies the confidence of the sample's assigned methylation class using a calibrated score between 0 and 1. The sum of all calibrated scores across all methylation classes is 1.0. A confident match is generally considered >0.9 and a poor match <0.5[4]. The 22 cases that underwent analysis with the DNA methylation classification algorithm corresponded to 6 AFH, 4 CCS, 8 GICCS, 1 ME, 3 Meso among the 80 samples that underwent methylation profiling.

### Affymetrix microarray gene expression analysis

Details of the microarray protocol were described previously[5,6]. RNA was isolated using RNAwiz RNA isolation reagent (Ambion) and run through a column with RNase-free DNase (Qiagen). Ten micrograms of labeled and fragmented cRNA were then hybridized onto a Human Genome U133A expression array (Affymetrix, Santa Clara, CA). Post-hybridization staining, washing, and scanning were done according to instructions from the manufacturer (Affymetrix). The raw expression data were derived using the Affymetrix Microarray Analysis 5.0 (MAS 5.0) software. The data were normalized using a scaling target intensity of 500 to account for differences in the global chip intensity. The expression values were transformed using the logarithm base two. Affymetrix U133A gene expression array analysis was performed in a total of 58 samples, including 3 AFH, 4 CCS, 1 GICCS, and compared to 44 soft tissue tumors of various histotypes (3 adult fibrosarcomas, 5 angiosarcomas, 3 leiomyosarcomas, 10 gastrointestinal stromal tumors, 3 myxoid liposarcomas, 6 paragangliomas, 4 small blue round cell tumors, 4 solitary fibrous tumors, 3 synovial sarcoma, 3 undifferentiated pleomorphic sarcomas) and 6 normal tissues (adrenal gland, brain, kidney, small intestine, stomach, testis). For differential gene expression analysis, a minimum cutoff of $\log_2FC$ (fold change) >1.0 and FDR adjusted $p < 0.01$ were used for $t$ test. We compared one histotype against all other tumors for each respective analysis. For example: CCS (4 cases) vs all others (54 cases) in one analysis, and AFH (3 cases) vs all others (55 cases) in a different analysis. Unsupervised hierarchical clustering was performed using the pheatmap R package version 1.0.12 with Ward's linkage and Euclidean distance for clustering.

### Integration of gene expression and methylation analysis

First, we performed differential gene expression and differential methylation analysis by setting a false discovery rate (FDR) adjusted $p$ value of 0.01 and a minimum $\log_2FC$ (fold change) of 1.0 for $t$ test, comparing one histotype against all other tumors each time (e.g., CCS vs all others, AFH vs all others). Thereafter, for integration of transcriptomic and methylation data, we matched all the genes that were both differentially expressed based on $\log_2FC$ >1.0 and FDR < 0.01 and differentially methylated based on $\log_2FC > 2.0$ and FDR < 0.01 for the CCS vs all others and AFH vs all others comparisons. Out of the 3 AFH, 4 CCS and 1 GICCS on the Affymetrix U133 microarray, 1 AFH and 2 CCS did not overlap with the samples used for the methylation array.

## RESULTS

### Clinicopathologic summary

A total of 137 cases were identified [76 females, 61 males, mean age 37 (range 2–86)], including: 40 CCS (29%), 36 AFH (26%), 20 GICCS (15%), 14 ME (10%), 10 HCCC (7%), 8 Meso (6%), 5 MMT (4%), 3 PPMS (2%), and 1 clear cell odontogenic carcinoma (CCOC) (1%) (Fig. 1A). The mean ages in HCCC, PPMS and CCOC were higher than those in AFH, CCS, GICCS, MMT, and ME (Table 1). As expected, the primary sites were predominantly soft tissue for AFH and CCS, gastrointestinal tract/pelvis for GICCS, brain for MMT, thoracic or abdominopelvic cavities for Meso and ME, lung for PPMS, and major and minor salivary glands for HCCC.

### Fusion types and transcript variants by diagnosis

The distribution of the *EWSR1/FUS* fusion partners, *ATF1*, *CREB1*, and *CREM*, was significantly different across different tumor types (chi-square $P < 0.0001$) (Fig. 1B). Specifically, *EWSR1::ATF1* fusions were the only fusion type in HCCC (100%) and the predominant fusion type in CCS (85%) and Meso (88%); *EWSR1::CREB1* fusions were the only fusion type in PPMS (100%) and the predominant fusion type in AFH (60%); *EWSR1/FUS::CREM* fusions were the predominant fusion type in ME (86%). *CREB1* and *CREM* fusions were equally distributed in MMT (40% each). *ATF1* and *CREB1* fusions were equally distributed in GICCS. The single case of CCOC had a *EWSR1::ATF1* fusion. Of the 137 cases, only 5 (4%) harbored *FUS* fusions: four were *FUS::CREM* fusions in ME, one was a *FUS::ATF1* fusion in a Meso.

The exon usage for the fusion transcript variants for each tumor type was derived from either MSK-Fusion and/or MSK-IMPACT testing and available in 48 cases (8 AFH, 18 CCS, 9 GICCS, 7 HCCC, 3 Meso, 1 PPMS, 2 ME) (Table 2). The predominant fusion transcript variants were *EWSR1*ex8::*ATF1*ex4 in CCS and GICCS; *EWSR1*ex7::*ATF1*ex5 and *EWSR1*ex7::*CREB1*ex7 in AFH; *EWSR1*ex11::*ATF1*ex3 in HCCC; *FUS*ex8::*CREM*ex5/7 for ME (Fig. 2). Supplementary Table 1 summarizes the CREB family fusion variants of various tumor types derived from our meta-analysis of published studies in comparison to those detected in the current cohort.
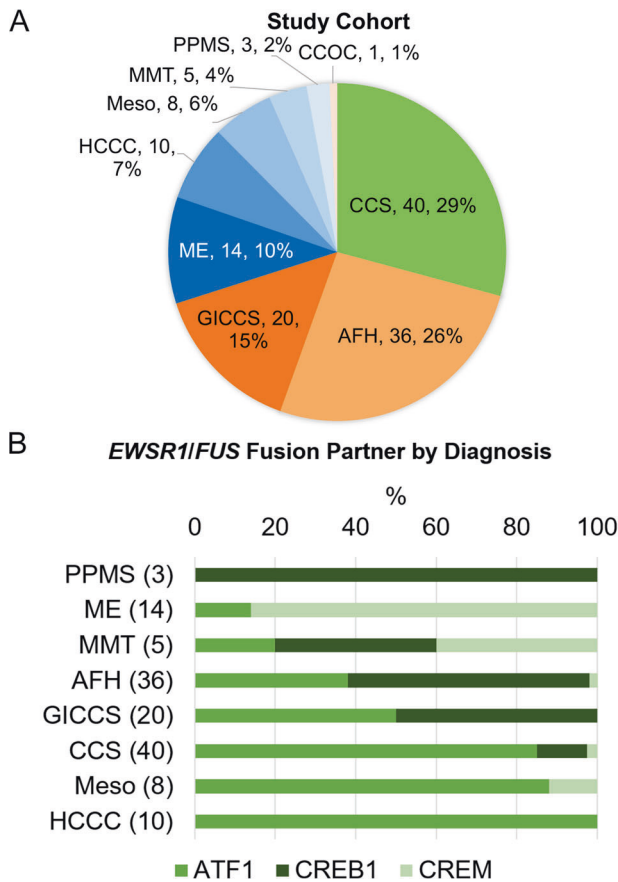
**Fig. 1 Distribution of tumor types and *EWSR1/FUS* fusion partners. A** Study cohort showing number of cases and percentages by tumor type. **B** Distribution of *EWSR1/FUS* fusion partners (*ATF1*, *CREB1*, *CREM*) by diagnosis (number of cases for each histotype indicated between parenthesis). Abbreviations—AFH angiomatoid fibrous histiocytoma, CCS clear cell sarcoma, CCOS clear cell odontogenic carcinoma, GICCS clear cell sarcoma-like tumor of gastrointestinal tract, HCCC hyalinizing clear cell carcinoma of salivary gland, ME malignant epithelioid neoplasm with predilection for mesothelial-lined cavities, Meso mesothelioma, PPMS: primary pulmonary myxoid sarcoma.

## Clinically significant recurrent genetic alterations

39 cases [6 AFH, 14 CCS, 9 GICCS, 5 HCCC, 3 Meso, 1 PMMS, 1 clear cell odontogenic carcinoma (CCOS)] were analyzed by MSK-IMPACT. Only clinically significant variants with OncoKB annotations (Chakravarty 2017) (or known recurrent hotspots) and secondary recurrent genetic alterations (events that occur >1 in our cohort) were included. Variants of unknown significance were excluded. Of the 39 cases that underwent targeted NGS testing, 18 (46%) had OncoKB mutations or copy number alterations (29 secondary genetic events in total), of which 15 (52%) were recurrent. Specifically, *TERT* promoter hotspot mutations ($n = 5$) and *CDKN2A* X51_splice and P81Lfs*30 mutations ($n = 2$) were mutually exclusive and identified in CCS only. Other secondary recurrent genetic alterations identified were: *TP53* R248Q and T155Pfs*15 mutations ($n = 2$, 1 CCS, 1 GICCS), 9p21.3 (*CDKN2A/CDKN2B*) copy number loss (homozygous deletion) ($n = 4$, 2 AFH, 1 CCS, 1 HCCC), and *DIS3* D479G and D488N mutations ($n = 2$, both GICCS) (Fig. 3A). No secondary recurrent genetic alterations were identified in any of the 3 Meso, 1 PMMS, or 1 CCOC. The type of secondary recurrent genetic alterations did not correlate with the *EWSR1/FUS* fusion partner type (Supplementary Fig. 1).

Interestingly, AFH cases with *CDKN2A/CDKN2B* homozygous deletion ($n = 2$, 33%) were exclusively found in metastatic cases, whereas the remaining *CDKN2A/CDKN2B* non-altered AFH cases

**Table 1.** Clinicopathologic summary of the study cohort.

| Diagnosis | Female, n (%) | Male, n (%) | Mean age in years (range) | Median tumor size in cm (range) | Top primary site | Metastasis, n (%) | Top metastatic site | Total |
|---|---|---|---|---|---|---|---|---|
| Angiomatoid fibrous histiocytoma | 19 (53) | 17 (47) | 28.3 (2–79) | 3.4 (1.0–10.5) | Lower extremities, upper extremities, head and neck, trunk | 4 (11) | Lung, bone, adrenal | 36 |
| Clear cell odontogenic carcinoma | 1 (100) | 0 | 57.0 | 2.7 | Head and neck | 0 | N/A | 1 |
| Clear cell sarcoma | 16 (40) | 24 (60) | 32.9 (7–71) | 4.7 (2.5–12.0) | Lower extremities, upper extremities | 18 (45) | Lymph node, lung | 40 |
| Clear cell sarcoma-like tumor of the gastrointestinal tract | 14 (70) | 6 (30) | 39.0 (18–76) | 4.5 (2.5–6.0) | Gastrointestinal tract | 8 (40) | Liver, abdominopelvic | 20 |
| Hyalinizing clear cell carcinoma of salivary gland | 8 (80) | 2 (20) | 67.6 (55–86) | 2.1 (1.3–3.3) | Salivary gland | 3 (30) | Lymph node, trunk, abdominopelvic | 10 |
| Malignant epithelioid neoplasm with predilection for mesothelial-lined cavities | 7 (50) | 7 (50) | 37.2 (9–63) | 9.0 (4.5–15.0) | Abdominopelvic | 3 (21) | Lymph node, liver abdominopelvic | 14 |
| Mesothelioma | 5 (62) | 3 (38) | 39.0 (15–78) | 3.8 (2.6–8.5) | Abdominopelvic, pleura | 2 (25) | Lymph node, abdominopelvic | 8 |
| Myxoid mesenchymal tumor | 3 (60) | 2 (40) | 27.0 (12–48) | 2.9 (2.8–3.0) | Brain | 0 | N/A | 5 |
| Primary pulmonary myxoid sarcoma | 3 (100) | 0 | 59.0 (43–82) | 1.4 | Lung | 1 (33) | Lymph node | 3 |
| Total | 76 | 61 | 36.4 (5–86) | 4.0 | | 39 (28) | | 137 |

**Table 2.** Distribution of the most prevalent fusion transcript variants by exon usage in the current study.

| Histotype | Fusion transcript variant | Number | Percentage |
|---|---|---|---|
| Angiomatoid fibrous histiocytoma (AFH) | *EWSR1::ATF1* ex7::ex5 | 3 | 37.5 |
| | *EWSR1::ATF1* ex7::ex7 | 1 | 12.5 |
| | *EWSR1::CREB1* ex7::ex7 | 3 | 37.5 |
| Clear cell sarcoma (CCS) | *EWSR1::ATF1* ex7::ex4 | 1 | 5.6 |
| | *EWSR1::ATF1* ex7::ex5 | 3 | 16.7 |
| | *EWSR1::ATF1* ex8::ex4 | 10 | 55.6 |
| | *EWSR1::ATF1* ex9::ex4 | 2 | 11.1 |
| | *EWSR1::CREB1* ex7::ex7 | 1 | 5.6 |
| | *EWSR1::CREM* ex8::ex7 | 1 | 5.6 |
| Clear cell sarcoma-like tumor of the gastrointestinal tract (GICCS) | *EWSR1::ATF1* ex7::ex5 | 1 | 11.1 |
| | *EWSR1::ATF1* ex8::ex4 | 5 | 55.6 |
| | *EWSR1::CREB1* ex6::ex6 | 1 | 11.1 |
| | *EWSR1::CREB1* ex7::ex6 | 1 | 11.1 |
| | *EWSR1::CREB1* ex7::ex7 | 1 | 11.1 |
| Hyalinizing clear cell carcinoma (HCCC) | *EWSR1::ATF1* ex7::ex4 | 1 | 14.3 |
| | *EWSR1::ATF1* ex8::ex4 | 1 | 14.3 |
| | *EWSR1::ATF1* ex9::ex2 | 1 | 14.3 |
| | *EWSR1::ATF1* ex10::ex3 | 1 | 14.3 |
| | *EWSR1::ATF1* ex11::ex3 | 3 | 42.9 |
| Malignant epithelioid neoplasm with predilection for mesothelial-lined cavities (ME) | *FUS::CREM* ex8::ex5 | 1 | 50.0 |
| | *FUS::CREM* ex8::ex7 | 1 | 50.0 |
| Mesothelioma (Meso) | *EWSR1::ATF1* ex7::ex5 | 1 | 33.3 |
| | *EWSR1::ATF1* ex13::ex5 | 1 | 33.3 |
| | *EWSR1::CREM* ex10::ex5 | 1 | 33.3 |

Transcripts: *ATF1* (NM_005171); *CREB1* (NM_134442); *CREM* (NM_181571); *EWSR1* (NM_005243); *FUS* (NM_004960).
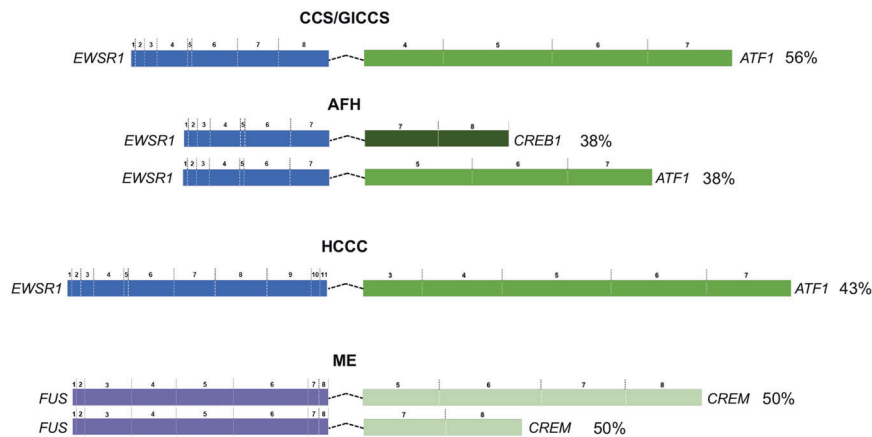


**Fig. 2   Schematics of predominant fusion transcript variants, for AFH, CCS, GICCS, HCCC, and ME. Exon numbers were based on canonical transcripts for each gene.** Percentage indicates frequency of the fusion transcript variant within the corresponding histotype subgroup. RefSeq accession number: *ATF1* (NM_005171); *CREB1* (NM_134442); *CREM* (NM_181571); *EWSR1* (NM_005432); *FUS* (NM_004960). Abbreviations —AFH angiomatoid fibrous histiocytoma, CCS clear cell sarcoma, GICCS clear cell sarcoma-like tumor of gastrointestinal tract, HCCC hyalinizing clear cell carcinoma of salivary gland, ME malignant epithelioid neoplasm with predilection for mesothelial-lined cavities, Meso mesothelioma.

were non-metastatic (Fig. 3B). On the other hand, CCS cases with *TERT* promoter mutations and *CDKN2A* loss-of-function mutations (frameshift and splice site mutations) ($n = 7$, 50%) were significantly correlated with decreased overall survival (Mantel Haenszel chi-square $P = 0.0196$) (Fig. 3C), with a median survival of 5.13 vs 22.85 months in non-altered CCS cases ($n = 7$, 50%). The presence of *DIS3* mutations were not correlated with metastatic nor survival status in GICCS.

**Methylation and gene expression correlation**
Gene expression profiling were performed on the Affymetrix U133A expression array comparing 3 AFH, 4 CCS cases, and 1 GICCS to a group of 44 soft tissue tumors of various histotypes and 6 normal tissue samples (Supplementary Fig. 2 and Supplementary Table 2). Methylation profile testing was performed comparing 7 AFH, 4 CCS, 4 GICCS to a group of 51 soft tissue tumors of various histotypes and 10 normal tissue
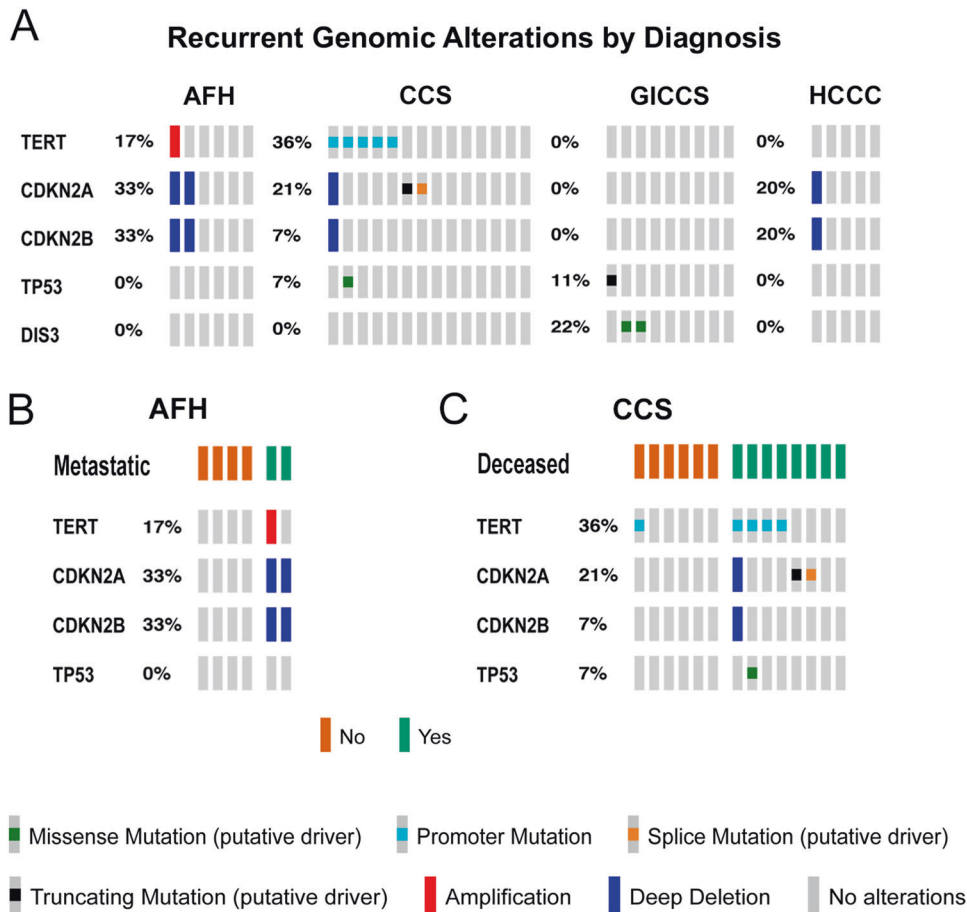
**Fig. 3** **Recurrent genomic alterations in AFH, CCS, GICCS, and HCCC. A** Recurrent genomic alterations identified by MSK-IMPACT, including OncoKB mutations and copy number alterations[84], in 6 AFH, 14 CCS, 9 GICCS, and 5 HCCC. Only genomic alteration events occurring >1 were included. **B** Presence of *TERT*, *CDKN2A*, and *CDKN2B* alterations in AFH with or without metastatic disease. **C** Presence of *TERT*, *CDKN2A*, *CDKN2B* and *TP53* alterations in living vs deceased CCS patients. Data generated from cBioPortal and visualized using OncoPrint[85]. Abbreviations—AFH angiomatoid fibrous histiocytoma, CCS clear cell sarcoma, GICCS clear cell sarcoma-like tumor of gastrointestinal tract, HCCC hyalinizing clear cell carcinoma of salivary gland.

samples on the 850k methylation array (Supplementary Table 3). The goal was to identify correlates between differential gene expression (1.5 $\log_2$ FC, FDR 0.01) and differential methylation (4 $\log_2$ FC and FDR 0.01) for *EWSR1::ATF1*-rearranged CCS and *EWSR1::CREB1*-rearranged AFH, respectively, in relation to other tumor types. Gene expression profiling revealed upregulation of *PMP22*, *MITF*, *SLC7A5*, *CDH19*, *WIPI1*, *FYN*, *PARVB*, and *PFKP* in CCS but not AFH, and upregulation of *SGK1*, *S100A4*, *XAF1* and *LY96* expression in AFH but not CCS. Additional methylation data from the study by Koelsche et al.[4] (8 AFH, 7 CCS, and soft tissue tumors of various histotypes and normal tissue samples) were retrieved and included in unsupervised t-SNE clustering analysis. Unsupervised clustering of methylation profiles showed that CREB family translocation tumors (AFH, CCS, GICCS, Meso) each form tight, distinct clusters that were nearby each other (Supplementary Fig. 3 and Supplementary Table 3).

Thereafter, differentially expressed genes were matched to CpG sites based on chromosomal locations. We matched all the genes that were both differentially expressed based on $\log_2$FC > 1.0 and FDR < 0.01 and differentially methylated based on $\log_2$FC > 2.0 and FDR < 0.01. We focused on upregulated genes with corresponding hypomethylation. Our analyses revealed genes (*MITF*, *CDH19*, *PARVB*, and *PFKP*) with increased expression and hypomethylation in CCS but not AFH (Fig. 4A), and genes (*S100A4*, *XAF1*) with increased

expression and hypomethylation in AFH but not CCS (Fig. 4B). *MITF* is involved in melanogenesis and overexpressed in CCS as part of its core gene signature[5,7]. *CDH19* and *PARVB* are involved in cell adhesion and were highly expressed in primary melanoma[8]. *S100A4* has been implicated in cell migration and cancer metastases[9]. *XAF1* is a proapoptotic tumor suppressor gene[10].

**Tumor type prediction by the sarcoma methylation classifier**
The DNA-methylation based sarcoma classification algorithm described in Koelsche et al.[4] was applied to 22 cases (6 AFH, 4 CCS, 8 GICCS, 1 ME, and 3 Meso) (Table 3). This algorithm was able to accurately match 100% of four CCS cases to the correct methylation class (calibrated score = 0.99 in all cases), but only 33% (2 of 6) of AFH cases (calibrated score = 0.75 and 0.33, respectively). GICCS was not a methylation class in the original classifier. Interestingly, the algorithm matched 1 GICCS to AFH (calibrated score 0.56) and 2 GICCS to CCS (calibrated score = 0.65 and 0.96, respectively).

**Survival analysis**
The overall survival across AFH, CCS, GICCS, HCCC was significantly different (log rank $P = 0.023$), with CCS associated with the worse survival (median survival 15 months), followed by HCCC (median survival 36 months) and then GICCS (median survival 43 months). All AFH patients remained alive across the follow-up period of 42 months (Fig. 5).
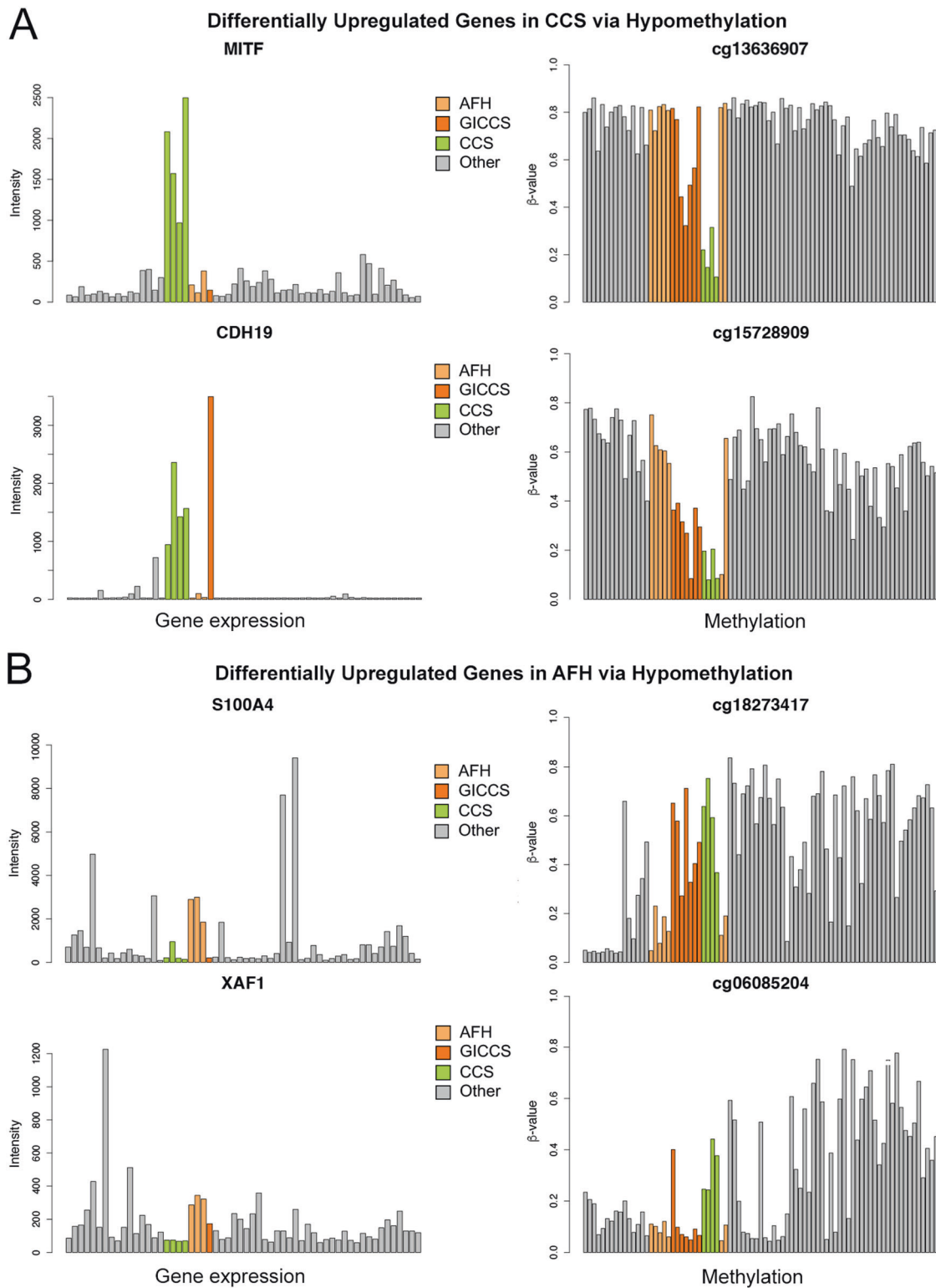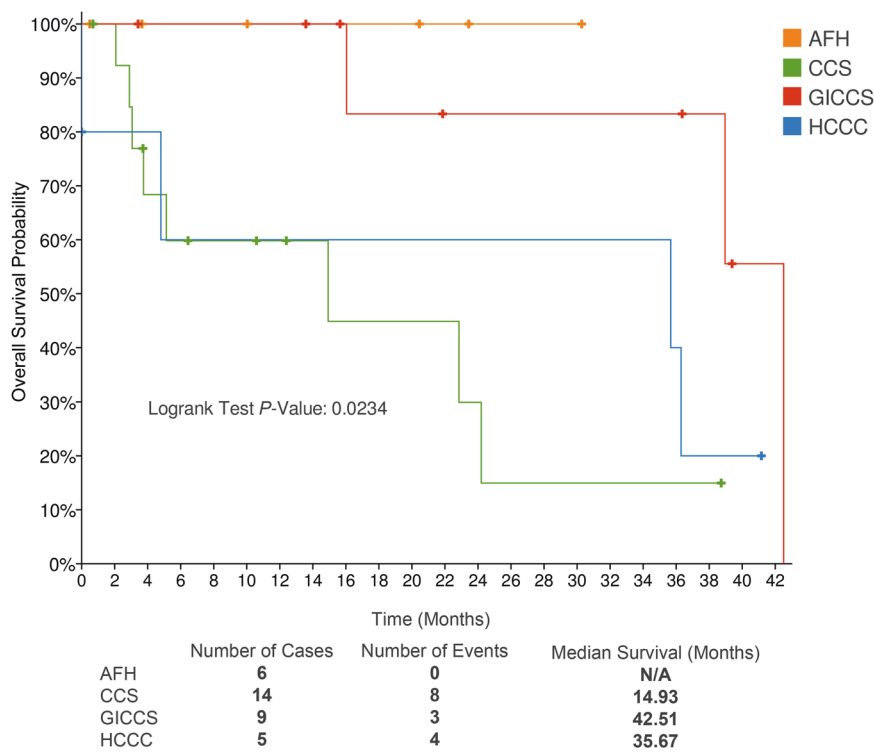
**Fig. 4 Differential gene upregulation corresponding to hypomethylation on matched CpG sites. A** CCS. **B** AFH. Affymetrix U133A was performed comparing 3 AFH, 4 CCS cases, and 1 GICCS to a group of 44 tumors of various histotypes and 6 normal tissues, using $\log_2$-fold change threshold of 1 and $P < 0.01$. Infinium 850k methylation array was performed comparing 7 AFH, 4 CCS, 4 GICCS to a group of 29 tumors of various histotypes and 8 normal tissues, using a $\log_2$-fold change threshold of 2 and $P < 0.01$. Differentially expressed genes were matched to CpG site identified by a unique cg identifier in the format of cg#. The numbers of CpG sites assigned to each of these 4 genes on the 850k array were as follows: 8 for *S100A4*, 14 for *XAF1*, 27 for *MITF*, and 3 for *CDH19*. Out of these, the numbers of CpG sites that showed negative correlation with gene expression were as follows: 3 for *S100A4*, 6 for *XAF1*, 3 for *MITF*, and 3 for *CDH19*. The most representative CpG site from each gene was displayed in this figure. Abbreviations—AFH angiomatoid fibrous histiocytoma, CCS clear cell sarcoma, GICCS clear cell sarcoma-like tumor of gastrointestinal tract.

**Table 3.** Tumor type prediction by sarcoma methylation classifier[a].

| Diagnosis | Age/Sex | Site | Fusion | Calibrated score | Matching methylation class |
|---|---|---|---|---|---|
| **AFH** | 21/M | groin | *EWSR1::CREB1* | 0.33 | **angiomatoid fibrous histiocytoma** |
| **AFH** | 16/M | scalp | *EWSR1::CREB1* | 0.75 | **angiomatoid fibrous histiocytoma** |
| AFH | 79/F | knee | *EWSR1::ATF1* | <0.3 | no matching methylation class |
| AFH | 22/F | inguinal | *EWSR1::CREB1* | <0.3 | no matching methylation class |
| AFH | 34/M | foot | *EWSR1::ATF1* | <0.3 | no matching methylation class |
| AFH | 17/M | axilla | *EWSR1::CREB1* | 0.74 | squamous cell carcinoma (cutaneous) |
| **CCS** | 20/F | heel | *EWSR1::ATF1* | 0.99 | **clear cell sarcoma of soft parts** |
| **CCS** | 30/M | knee | *EWSR1::ATF1* | 0.99 | **clear cell sarcoma of soft parts** |
| **CCS** | 24/M | arm | *EWSR1::ATF1* | 0.99 | **clear cell sarcoma of soft parts** |
| **CCS** | 46/F | hip | *EWSR1::ATF1* | 0.99 | **clear cell sarcoma of soft parts** |
| **GI CCS** | 42/F | small bowel | *EWSR1::CREB1* | 0.56 | **angiomatoid fibrous histiocytoma** |
| **GI CCS** | 47/F | small bowel | *EWSR1::CREB1* | 0.65 | **clear cell sarcoma of soft parts** |
| **GI CCS** | 57/M | stomach | *EWSR1::CREB1* | 0.96 | **clear cell sarcoma of soft parts** |
| GI CCS | 42/F | small bowel | *EWSR1::CREB1* | 0.51 | neurofibroma (plexiform) |
| GI CCS | 19/F | mesentery | *EWSR1::ATF1* | <0.3 | no matching methylation class |
| GI CCS | 76/F | colon | *EWSR1::CREB1* | <0.3 | no matching methylation class |
| GI CCS | 18/F | small bowel | *EWSR1::ATF1* | <0.3 | no matching methylation class |
| GI CCS | 25/M | stomach | *EWSR1::CREM* | 0.68 | sclerosing epithelioid fibrosarcoma |
| ME | 20/F | peri-rectal | *EWSR1::CREM* | <0.3 | no matching methylation class |
| Meso | 26/F | peritoneal | *FUS::ATF1* | <0.3 | no matching methylation class |
| Meso | 34/F | pleura | *EWSR1::ATF1* | <0.3 | no matching methylation class |
| Meso | 79/F | mediastinum | *EWSR1::ATF1* | <0.3 | no matching methylation class |

*AFH* angiomatoid fibrous histiocytoma, *CCS* clear cell sarcoma, *GICCS* clear cell sarcoma-like tumor of gastrointestinal tract, *ME* malignant epithelioid neoplasm with predilection for mesothelial-lined cavities, *Meso* mesothelioma.
[a]Percentage matched (highlighted in bold face): AFH 33.3%, CCS 100%, GICCS/ME/meso (methylation class doesn't exist in the classifier).



| | Number of Cases | Number of Events | Median Survival (Months) |
|---|---|---|---|
| AFH | **6** | **0** | **N/A** |
| CCS | **14** | **8** | **14.93** |
| GICCS | **9** | **3** | **42.51** |
| HCCC | **5** | **4** | **35.67** |

**Fig. 5 Comparison of overall survival in 6 AFH, 14 CCS, 9 GICCS, and 5 HCCC.** Median survival time (months) for each tumor type listed beneath Kaplan–Meier curves. Hazard ratios compared using log-rank analysis. Abbreviations—AFH angiomatoid fibrous histiocytoma, CCS clear cell sarcoma, GICCS clear cell sarcoma-like tumor of gastrointestinal tract, HCCC hyalinizing clear cell carcinoma of salivary gland.

1062

## DISCUSSION

The *EWSR1*/FUS::CREB family of translocation-associated tumors encompasses a wide and heterogenous clinicopathologic spectrum. To understand the pathogenesis that sets them apart, we performed comprehensive genomic analysis of fusion variants, secondary recurrent genetic alterations (mutations, copy number alterations), gene expression and methylation profiles across a large cohort of *EWSR1*::CREB family of translocation-associated tumors, with emphasis on AFH, CCS, GICCS, and HCCC.

Although the analysis of fusion transcript variants in our cohort largely paralleled the published literature, some new interesting findings emerged. For AFH, the most common reported fusion transcript variant is *EWSR1*::CREB1 (ex7-ex7) (58%)[7,11–15]. However, we identified a significant proportion (39%) of AFH cases with *EWSR1*::ATF1 (largely ex7-ex5). A minority (3%) of AFH harbored *EWSR1*::CREM fusions. Interestingly, MMT[16–21], which remains disputed by some authors to be related to a myxoid, intracranial variant of AFH[22–27], harbor roughly equal proportions of *EWSR1*::CREM and *EWSR1*::CREB1 fusions, with a minority harboring *EWSR1*::ATF1. For CCS, the predominant fusion transcript is *EWSR1*ex8::ATF1ex4[15,28–34]. This pattern is mirrored by a subtype of Meso, initially described by our group and occurs in younger patients without asbestos exposure history, which are driven predominantly by *EWSR1*::ATF1ex5[35–37]. Of interest, in contrast to prior data, GICCS showed similar proportions of *EWSR1*::ATF1 (mostly ex8-ex4) and *EWSR1*::CREB1 fusions[5,34,38]. On the other hand, the recently described distinct tumor type, so-called "malignant epithelioid neoplasm with predilection for mesothelial-lined cavities"[39] and subsequently validated by Shibayama et al.[40], most commonly harbor either fusions between *EWSR1* or *FUS* and exon 7 of *CREM*. In contrast, PPMS is almost exclusively driven by *EWSR1*::CREB1 (mostly ex7-ex7)[41–48] except for a rare case with *EWSR1*::ATF1[49]. Some authors proposed that PPMS and AFH exist on a morphologic and molecular spectrum[43,49]. Finally, both HCCC[50–55] and CCOC[56–60] harbor only *EWSR1*::ATF1, supporting the notion that HCCC and CCOC are likely related tumors. Nevertheless, it is evident from our meta-analysis of the published literature and from the current study that there is significant intertumoral overlap as well as intratumoral heterogeneity of fusion transcript variants and exon usage across the different CREB family translocation tumors. Here, intratumoral heterogeneity refers to variation of fusion transcript variants, e.g., *EWSR1*::ATF1 and *EWSR1*::CREB1 in GICCS, and exon usage within the same histotype, e.g., *FUS*::CREM exon 5 and *FUS*::CREM exon 7 in ME.

This is the first study to report secondary recurrent genomic alterations in CCS, AFH and GICCS. In CCS, we identified the presence of recurrent *TERT* promoter and *CDKN2A* hotspot mutations, which were mutually exclusive but in combination strongly associated with worse overall survival. *TERT* promoter somatic mutations and amplifications are frequently found across multiple tumor types[61,62]. In soft tissue tumors, *TERT* promoter mutations have been identified in myxoid liposarcomas[63], atypical fibroxanthoma/pleomorphic dermal sarcomas[64], chondrosarcomas[65], and solitary fibrous tumors[66]; this is reported to be associated with a worse prognosis in the latter. Our findings suggest that *TERT* promoter and *CDKN2A* mutations may serve as prognostic biomarkers for worse survival in CCS.

In AFH, we identified *CDKN2A/CDKN2B* homozygous deletions exclusively amongst cases with metastasis. Genomic profiling of multiple sarcoma types has revealed secondary recurrent *CDKN2A* alterations[67,68], with a role suggested as a biomarker for poor prognosis[67]. Compared to other CREB family translocations tumors, AFH is a soft tissue tumor of borderline malignant potential and a relatively good prognosis; metastasis is usually <2%. In fact, all the patients whose AFH were sequenced in our cohort remain alive at the time of reporting. Our finding of *CDKN2A/CDKN2B* deletions in the two AFH cases with biopsy-

proven metastasis, but not in the non-metastatic AFH cases, raises the possibility of *CDKN2A/CDKN2B* deletion testing as a biomarker for metastatic potential. Although not a recurrent abnormality in this cohort, one of the metastatic AFH case showed a co-existing *BRAF* V600E mutation which was confirmed by immunohistochemistry to have diffuse and strong VE1 expression. This was the only case in our cohort to have a *BRAF* mutation detected.

Gene expression profiling revealed differential gene expression in AFH vs CCS, which clustered in distinct genomic groups by unsupervised analysis. A number of genes involved in melanocyte regulation and cellular membrane/migration were upregulated in CCS compared to AFH, including *PMP22*, *MITF*, *SLC7A5*, *CDH19*, *WIPI1*, *FYN*, *PARVB*, and *PFKP*, while upregulation of *SGK1*, *S100A4*, *XAF1* and *LY96* mRNA expression was detected in AFH but not CCS. An expression profiling analysis of CCS cell lines revealed upregulation of *S100A11* (encoding for S100 protein), *MITF* (microphthalmia-associated transcription factor), and *Pmel17* (*SILV*) (silver mouse homologue-like melanosomal protein detected by the IHC marker HMB45)[69]. Moreover, in an in vitro CCS induced pluripotent stem cell model, Komura et al. reported expression of several Schwann cell marker genes, such as *P75^{NTR}*, *S100b*, *Mbp*, *Plp1*, and *Pmp22*[70]. They proposed that S100-expressing peripheral nerve cells could be a cell of origin for *EWS/ATF1*-induced CCS. In a recent study using human embryonic stem (hES) cell models, hES cells driven by *EWSR1*::CREB1 and *EWSR1*::ATF1 fusions recapitulate the core gene signatures, respectively, of AFH (*SGK1* and *MXRA5* upregulation) and GICCS (*SGK1*, *MXRA5*, *SOX10*, and *DUSP4* upregulation)[71]. Our gene expression profiling of patient samples validates a subset of the findings of these preclinical studies.

Our methylation profiling and multidimensionality reduction clustering analysis revealed that CREB family translocation-associated tumors (AFH, CCS, GICCS, Meso) form neighboring but tight clusters that were distinct from other soft tissue tumor types and normal tissue. When matching the differentially expressed genes to the corresponding methylation probes/CpG sites, we found significant correlations between upregulated genes that were hypomethylated in CCS but not AFH. These genes included *MITF*, *CDH19*, *PARVB*, and *PFKP* in CCS. *MITF* is involved in melanogenesis and found to be overexpressed in CCS as part of its core gene signature, but not in AFH or GICCS[5,7]. More recently, a Cre-loxP-induced *Ewsr1*::*Atf1*-driven CCS model demonstrated that *Mitf* and *Myc* can contribute to sarcomagenesis[72]. Both *CDH19* and *PARVB* are involved in cell adhesion and were highly expressed in primary melanoma, associated with worse survival[8]. It is interesting how they were found to show increased expression and hypomethylation in CCS in our study. On the other hand, we identified upregulation and hypomethylation of *S100A4* and *XAF1* in AFH but not CCS. S100A4 protein is a member of the S100 calcium binding protein family, also known as metastasin, and has been implicated in cell migration and cancer metastases[9]. *XAF1* is a proapoptotic, interferon-stimulated tumor suppressor gene that suppresses tumorigenesis[10]. While *XAF1* is usually hypermethylated and down-regulated in most cancers, it was found to be paradoxically hypomethylated in glioblastoma with adaptive temozolomide resistance[73]. These findings serve as a proof-of-concept example of how integrative gene expression and methylation profiling may provide interesting biological insights into the different pathogenesis underlying tumors sharing the same driver gene fusions. Integrated DNA methylation and gene expression studies have been performed in Ewing sarcoma[74], pediatric rhabdomyosarcomas[75], myxoid, dedifferentiated, and pleomorphic liposarcomas[76], which identified sets of genes with inverse methylation and gene expression relationship. In a comprehensive molecular and genomic study of undifferentiated sarcomas (USARC), DNA methylation profiling failed to identify distinct USARC subgroups and did not correlate with

gene expression, but showed *MSH2* and *TERT* promoter hypermethylation[77]. On the other hand, DNA methylation profiling also revealed epigenetic heterogeneity within the same tumor type, e.g., Ewing sarcoma[78]. Unfortunately, the sample size of individual tumor types used for methylation profiling in the current study is insufficient to perform differential methylation analysis within the same tumor type, which could be explored in future studies.

Genome-wide DNA methylation profiling has largely been performed for tumor classification purposes in a wide range of mesenchymal tumors, with varying degree of success. These include: benign and malignant nerve sheath tumors[79], osteosarcomas[80], undifferentiated small round blue cell tumors[81], *CIC*-rearranged undifferentiated sarcomas[82]. Most recently, a Random Forest machine learning sarcoma classifier from the German Cancer Research Center (DKFZ) in Heidelberg were developed to classify a wide spectrum of 66 soft tissue and bone tumors using a large reference and validation cohort[4]. The limitations of using methylation profiling alone to differentiate soft tissue tumors were illustrated by the inability of the Heidelberg methylation classifier to accurately classify tumor entities in our cohort, with the exception of CCS. There are several major shortcomings to the applicability of this methylation classifier for soft tissue tumors with *EWSR1/FUS* fusions with CREB family transcription factors. First, several tumor types, including GICCS and Meso, were not included in the reference cohort that was used to develop the classifier. Second, although the reference cohort included 8 cases of AFH, only 1 case was used in the validation cohort, which was misclassified as desmoplastic small round cell tumor[4]. In our study, the classifier was able to correctly classify one-third of the AFH cases. On the other hand, the methylation classifier performed very well, both in the Koelsche et al study and in our experience, in the classification of CCS: classifying 100% of the cases correctly. It is also interesting that when we applied the classifier to GICCS, 2 cases were classified as CCS and 1 case as AFH, illustrating their overlapping methylation profiling as described above. All 3 of these GICCS cases were located in the gastrointestinal tract (1 stomach, 2 small bowel), and were diffusely and strongly positive for S100 and negative for HMB45. The combined clinical and immunohistochemical profile essentially excludes CCS and AFH. These findings highlight the existing limitation of methylation profiling in soft tissue tumor classification, which may require further algorithm refinement as well as larger reference and validation cohorts[83].

In addition to these molecular mechanisms, the nature of the initial stem cell host in which the fusion, and its degree of commitment/plasticity, arose may also play a significant role in ultimate tumor type (i.e., depending on location/extent of totipotency). These are interesting questions that are beyond the scope of the current study. Recent studies using *Cre* inducible mouse and human embryonic stem cell models have begun to address these questions[71,72].

The lack of consistency in the sample sizes of the cases with each technique is a major drawback of our paper. Further studies focusing on specific molecular profiling techniques with deeper genomic characterization utilizing a larger sample size of some of the rarer histotypes would be beneficial to validate or expand on our findings.

In conclusion, our comprehensive genomic profiling of *EWSR1/FUS::CREB* translocation-associated tumors uncover fusion transcript variant heterogeneity, prognostically significant secondary recurrent genetic alterations, and differentially hypomethylated and upregulated genes. These findings underscore the utility of integrative genomic approaches in the study of translocation-associated tumors with diverse clinicopathologic features, and whether some of the entities in this family could be unified under the same morphologic/molecular spectrum (e.g., CCS and GICCS, AFH and PPMS).

## REFERENCES
1. Zehir, A. et al. Mutational landscape of metastatic cancer revealed from prospective clinical sequencing of 10,000 patients. *Nat. Med.* **23**, 703–713 (2017).
2. Benayed, R. et al. High Yield of RNA sequencing for targetable kinase fusions in lung adenocarcinomas with no mitogenic driver alteration detected by DNA sequencing and low tumor mutation burden. *Clin. Cancer Res.* **25**, 4712–4722 (2019).
3. Benhamida, J. K. et al. Reliable clinical MLH1 promoter hypermethylation assessment using a high-throughput genome-wide methylation array platform. *J. Mol. Diagn.* **22**, 368–375 (2020).
4. Koelsche, C. et al. Sarcoma classification by DNA methylation profiling. *Nat. Commun.* **12**, 498 (2021).
5. Antonescu, C. R., Nafa, K., Segal, N. H., Dal Cin, P. & Ladanyi, M. EWS-CREB1: a recurrent variant fusion in clear cell sarcoma–association with gastrointestinal location and absence of melanocytic differentiation. *Clin. Cancer Res.* **12**, 5356–5362 (2006).
6. Huang, S. C. et al. Frequent HRAS mutations in malignant ectomesenchymoma: overlapping genetic abnormalities with embryonal rhabdomyosarcoma. *Am. J. Surg. Pathol.* **40**, 876–885 (2016).
7. Antonescu, C. R. et al. EWSR1-CREB1 is the predominant gene fusion in angiomatoid fibrous histiocytoma. *Genes Chromosomes Cancer* **46**, 1051–1060 (2007).
8. Eriksson, J. et al. Gene expression analyses of primary melanomas reveal CTHRC1 as an important player in melanoma progression. *Oncotarget* **7**, 15065–15092 (2016).
9. Helfman, D. M., Kim, E. J., Lukanidin, E. & Grigorian, M. The metastasis associated protein S100A4: role in tumour progression and metastasis. *Br. J. Cancer* **92**, 1955–1958 (2005).
10. Liston, P. et al. Identification of XAF1 as an antagonist of XIAP anti-Caspase activity. *Nat. Cell Biol.* **3**, 128–133 (2001).
11. Waters, B. L., Panagopoulos, I. & Allen, E. F. Genetic characterization of angiomatoid fibrous histiocytoma identifies fusion of the FUS and ATF-1 genes induced by a chromosomal translocation involving bands 12q13 and 16p11. *Cancer Genet. Cytogenet.* **121**, 109–116 (2000).
12. Raddaoui, E., Donner, L. R. & Panagopoulos, I. Fusion of the FUS and ATF1 genes in a large, deep-seated angiomatoid fibrous histiocytoma. *Diagn. Mol. Pathol.* **11**, 157–162 (2002).
13. Hallor, K. H. et al. Fusion of the EWSR1 and ATF1 genes without expression of the MITF-M transcript in angiomatoid fibrous histiocytoma. *Genes Chromosomes Cancer* **44**, 97–102 (2005).
14. Rossi, S. et al. EWSR1-CREB1 and EWSR1-ATF1 fusion genes in angiomatoid fibrous histiocytoma. *Clin. Cancer Res.* **13**, 7322–7328 (2007).
15. Yoshida, A. et al. Expanding the phenotypic spectrum of mesenchymal tumors harboring the EWSR1-CREM fusion. *Am. J. Surg. Pathol.* **43**, 1622–1630 (2019).
16. Kao, Y. C. et al. EWSR1 fusions with CREB family transcription factors define a novel myxoid mesenchymal tumor with predilection for intracranial location. *Am. J. Surg. Pathol.* **41**, 482–490 (2017).
17. Sciot, R. et al. Primary myxoid mesenchymal tumour with intracranial location: report of a case with a EWSR1-ATF1 fusion. *Histopathology* **72**, 880–883 (2018).
18. Komatsu, M. et al. Intracranial myxoid mesenchymal tumor with EWSR1-CREB1 gene fusion: a case report and literature review. *Brain Tumor Pathol.* **37**, 76–80 (2020).
19. Ballester, L. Y. et al. Intracranial myxoid mesenchymal tumor with EWSR1-ATF1 fusion. *J. Neuropathol. Exp. Neurol.* **79**, 347–351 (2020).
20. Valente Aguiar, P., Pinheiro, J., Lima, J., Vaz, R. & Linhares, P. Myxoid mesenchymal intraventricular brain tumour with EWSR1-CREB1 gene fusion in an adult woman. *Virchows Arch.* **478**, 1019–1024 (2021).
21. Ward, B., Wang, C. P., Macaulay, R. J. B. & Liu, J. K. C. Adult intracranial myxoid mesenchymal tumor with EWSR1-ATF1 gene fusion. *World Neurosurg.* **143**, 91–96 (2020).
22. Bale, T. A. et al. Intracranial myxoid mesenchymal tumors with EWSR1-CREB family gene fusions: myxoid variant of angiomatoid fibrous histiocytoma or novel entity? *Brain Pathol.* **28**, 183–191 (2018).
23. Sloan, E. A. et al. Intracranial mesenchymal tumor with FET-CREB fusion-A unifying diagnosis for the spectrum of intracranial myxoid mesenchymal tumors and angiomatoid fibrous histiocytoma-like neoplasms. *Brain Pathol.* **31**, 12918 (2021).
24. Tan N. J. H., et al. Intracranial myxoid angiomatoid fibrous histiocytoma with 'classic' histology and EWSR1-CREM fusion providing insight for reconciliation with intracranial myxoid mesenchymal tumors. *Neuropathology* **41**, 306–314 (2021).

25. Dunham, C., Hussong, J., Seiff, M., Pfeifer, J. & Perry, A. Primary intracerebral angiomatoid fibrous histiocytoma: report of a case with a t (12; 22) (q13; q12) causing type 1 fusion of the EWS and ATF-1 genes. *Am. J. Surg. Pathol.* **32**, 478–484 (2008).

26. Gareton, A. et al. ESWR1-CREM fusion in an intracranial myxoid angiomatoid fibrous histiocytoma-like tumor: A case report and literature review. *J. Neuropathol. Exp. Neurol.* **77**, 537–541 (2018).

27. Konstantinidis, A. et al. Intracranial angiomatoid fibrous histiocytoma with EWSR1-CREB family fusions: a report of 2 pediatric cases. *World Neurosurg* **126**, 113–119 (2019).

28. Antonescu, C. R. et al. Molecular diagnosis of clear cell sarcoma: detection of EWS-ATF1 and MITF-M transcripts and histopathological and ultrastructural analysis of 12 cases. *J. Mol. Diagn.* **4**, 44–52 (2002).

29. Panagopoulos, I. et al. Molecular genetic characterization of the EWS/ATF1 fusion gene in clear cell sarcoma of tendons and aponeuroses. *Int. J. Cancer* **99**, 560–567 (2002).

30. Coindre, J. M. et al. Diagnosis of clear cell sarcoma by real-time reverse transcriptase-polymerase chain reaction analysis of paraffin embedded tissues: clinicopathologic and molecular analysis of 44 patients from the French sarcoma group. *Cancer* **107**, 1055–1064 (2006).

31. Hisaoka, M. et al. Clear cell sarcoma of soft tissue: a clinicopathologic, immunohistochemical, and molecular analysis of 33 cases. *Am. J. Surg. Pathol.* **32**, 452–460 (2008).

32. Wang, W. L. et al. Detection and characterization of EWSR1/ATF1 and EWSR1/CREB1 chimeric transcripts in clear cell sarcoma (melanoma of soft parts. *Mod. Pathol.* **22**, 1201–1209 (2009).

33. Jakubauskas, A. et al. Discovery of two novel EWSR1/ATF1 transcripts in four chimerical transcripts-expressing clear cell sarcoma and their quantitative evaluation. *Exp. Mol. Pathol.* **90**, 194–200 (2011).

34. Segawa, K. et al. Detection of specific gene rearrangements by fluorescence in situ hybridization in 16 cases of clear cell sarcoma of soft tissue and 6 cases of clear cell sarcoma-like gastrointestinal tumor. *Diagn. Pathol.* **13**, 73 (2018).

35. Desmeules, P. et al. A subset of malignant mesotheliomas in young adults are associated with recurrent EWSR1/FUS-ATF1 fusions. *Am. J. Surg. Pathol.* **41**, 980–988 (2017).

36. Ajelero, O., Zhang, P. L., Collingwood, R. & Fortuna, D. A rare case of malignant peritoneal mesothelioma with EWSR-ATF1 fusion transcription and unusual immunophenotype. *Hum. Pathol. Case Rep.* **25**, 200542 (2021).

37. Ren, H. et al. Malignant mesothelioma with EWSR1-ATF1 fusion in two adolescent male patients. *Pediatr. Dev. Pathol.* **12**, 10935266211021222 (2021).

38. Stockman, D. L. et al. Malignant gastrointestinal neuroectodermal tumor: clinicopathologic, immunohistochemical, ultrastructural, and molecular analysis of 16 cases with a reappraisal of clear cell sarcoma-like tumors of the gastrointestinal tract. *Am. J. Surg. Pathol.* **36**, 857–868 (2012).

39. Argani, P. et al. EWSR1/FUS-CREB fusions define a distinctive malignant epithelioid neoplasm with predilection for mesothelial-lined cavities. *Mod. Pathol.* **33**, 2233–2243 (2020).

40. Shibayama T., et al Cytokeratin-positive malignant tumor in the abdomen with EWSR1/FUS-CREB fusion: a clinicopathologic study of 8 cases. *Am. J. Surg. Pathol.* **46**, 134–146 (2022).

41. Thway, K. et al. Primary pulmonary myxoid sarcoma with EWSR1-CREB1 fusion: a new tumor entity. *Am. J. Surg. Pathol.* **35**, 1722–1732 (2011).

42. Matsukuma, S. et al. Primary pulmonary myxoid sarcoma with EWSR1-CREB1 fusion, resembling extraskeletal myxoid chondrosarcoma: case report with a review of Literature. *Pathol. Int.* **62**, 817–822 (2012).

43. Smith, S. C. et al. At the intersection of primary pulmonary myxoid sarcoma and pulmonary angiomatoid fibrous histiocytoma: observations from three new cases. *Histopathology* **65**, 144–146 (2014).

44. Jeon, Y. K., Moon, K. C., Park, S. H. & Chung, D. H. Primary pulmonary myxoid sarcomas with EWSR1-CREB1 translocation might originate from primitive peribronchial mesenchymal cells undergoing (myo)fibroblastic differentiation. *Virchows Arch* **465**, 453–461 (2014).

45. Yanagida, R., Balzer, B. L., Mckenna, R. J. & Fuller, C. B. Primary pulmonary myxoid sarcoma, a potential mimic of metastatic extraskeletal myxoid chondrosarcoma. *Pathology* **49**, 792–794 (2017).

46. Prieto-Granada, C. N., Ganim, R. B., Zhang, L., Antonescu, C. & Mueller, J. Primary pulmonary myxoid sarcoma: a newly described entity-report of a case and review of the literature. *Int. J. Surg. Pathol.* **25**, 518–525 (2017).

47. Chen, Z., Yang, Y., Chen, R., Ng, C. S. & Shi, H. Primary pulmonary myxoid sarcoma with EWSR1-CREB1 fusion: a case report and review of the literature. *Diagn. Pathol.* **15**, 15 (2020).

48. Koelsche, C. et al. Primary pulmonary myxoid sarcoma with an unusual gene fusion between exon 7 of EWSR1 and exon 5 of CREB1. *Virchows Arch* **476**, 787–791 (2020).

49. Gui, H., Sussman, R. T., Jian, B., Brooks, J. S. & Zhang, P. J. L. Primary pulmonary myxoid sarcoma and myxoid angiomatoid fibrous histiocytoma: a unifying continuum with shared and distinct features. *Am. J. Surg. Pathol.* **44**, 1535–1540 (2020).

50. Antonescu, C. R. et al. EWSR1-ATF1 fusion is a novel and consistent finding in hyalinizing clear-cell carcinoma of salivary gland. *Genes Chromosomes Cancer* **50**, 559–570 (2011).

51. Nakano, T. et al. Hyalinizing clear cell carcinoma with EWSR1-ATF1 fusion gene: report of three cases with molecular analyses. *Virchows Arch* **466**, 37–43 (2015).

52. Chapman, E. et al. Molecular profiling of hyalinizing clear cell carcinomas revealed a subset of tumors harboring a novel EWSR1-CREM fusion: report of 3 cases. *Am. J. Surg. Pathol.* **42**, 1182–1189 (2018).

53. Hirose, K. et al. Clear cell carcinoma of palatal minor salivary gland harboring a novel EWSR1-ATF1 fusion gene: report of a case and review of the literature. *Head Neck Pathol.* **15**, 676–681 (2021).

54. Nojima S., et al. Clear cell carcinoma in the oral cavity with three novel types of EWSR1-ATF1 translocation: a case report. *Head Neck Pathol.* (2021)

55. Heft Neal, M. E. et al. Integrative sequencing discovers an ATF1-motif enriched molecular signature that differentiates hyalinizing clear cell carcinoma from mucoepidemoid carcinoma. *Oral Oncol.* **117**, 105270 (2021).

56. Bilodeau, E. A. et al. Clear cell odontogenic carcinomas show EWSR1 rearrangements: a novel finding and a biological link to salivary clear cell carcinomas. *Am. J. Surg. Pathol.* **37**, 1001–1005 (2013).

57. Yancoskie, A. E. et al. EWSR1 and ATF1 rearrangements in clear cell odontogenic carcinoma: presentation of a case. *Oral Surg. Oral Med. Oral Pathol. Oral Radio* **118**, 115–118 (2014).

58. Vogels, R. et al. Clear cell odontogenic carcinoma: occurrence of EWSR1-CREB1 as alternative fusion gene to EWSR1-ATF1. *Head Neck Pathol.* **13**, 225–230 (2019).

59. Santana, T., Andrade, F. L., Sousa Melo, M. C., Rocha, G. B. L. & Trierveiler, M. Clear cell odontogenic carcinoma harboring the EWSR1-ATF1 fusion gene: report of a rare case. *Head Neck Pathol.* **14**, 847–851 (2020).

60. Breik O., et al. Clear cell odontogenic carcinoma: first report of novel EWSR1-CREM fusion gene in case of long-term misdiagnosis. *Head Neck Pathol.* (2021).

61. Bell, R. J. et al. Understanding TERT promoter mutations: a common path to immortality. *Mol. Cancer Res.* **14**, 315–323 (2016).

62. Gupta, S. et al. A Pan-Cancer Study of Somatic TERT promoter mutations and amplification in 30,773 tumors profiled by clinical genomic sequencing. *J. Mol. Diagn.* **23**, 253–263 (2021).

63. Koelsche, C. et al. TERT promoter hotspot mutations are recurrent in myxoid liposarcomas but rare in other soft tissue sarcoma entities. *J. Exp. Clin. Cancer Res.* **33**, 33 (2014).

64. Griewank, K. G. et al. TERT promoter mutations are frequent in atypical fibroxanthomas and pleomorphic dermal sarcomas. *Mod. Pathol.* **27**, 502–508 (2014).

65. Zhang Y., et al. TERT promoter mutation is an objective clinical marker for disease progression in chondrosarcoma. *Mod. Pathol.* (2021).

66. Bahrami, A. et al. TERT promoter mutations and prognosis in solitary fibrous tumor. *Mod. Pathol.* **29**, 1511–1522 (2016).

67. Bui, N. Q. et al. A clinico-genomic analysis of soft tissue sarcoma patients reveals CDKN2A deletion as a biomarker for poor prognosis. *Clin. Sarcoma Res.* **9**, 12 (2019).

68. Groisberg, R. et al. Clinical genomic profiling to identify actionable alterations for investigational therapies in patients with diverse sarcomas. *Oncotarget* **8**, 39254–39267 (2017).

69. Schaefer, K. L. et al. Expression profiling of t (12; 22) positive clear cell sarcoma of soft tissue cell lines reveals characteristic up-regulation of potential new marker genes including ERBB3. *Cancer Res.* **64**, 3395–3405 (2004).

70. Komura, S. et al. Cell-type dependent enhancer binding of the EWS/ATF1 fusion gene in clear cell sarcomas. *Nat. Commun.* **10**, 3999 (2019).

71. Vanoli F., et al. Generation of human embryonic stem cell models to exploit the EWSR1-CREB fusion promiscuity as a common pathway of transformation in human tumors. *Oncogene* https://doi.org/10.1038/s41388-021-01843-0 (2021).

72. Panza, E. et al. The clear cell sarcoma functional genomic landscape. *J. Clin. Invest.* **131**, 146301 (2021).

73. Wu, Q. et al. Paradoxical epigenetic regulation of XAF1 mediates plasticity towards adaptive resistance evolution in MGMT-methylated glioblastoma. *Sci. Rep.* **9**, 14072 (2019).

74. Patel, N. et al. DNA methylation and gene expression profiling of Ewing sarcoma primary tumors reveal genes that are potential targets of epigenetic inactivation. *Sarcoma* **2012**, 498472 (2012).

75. Mahoney, S. E. et al. methylation studies suggest distinct DNA methylation patterns in pediatric embryonal and alveolar rhabdomyosarcomas. *Epigenetics* **7**, 400–408 (2012).

76. Renner, M. et al. Integrative DNA methylation and gene expression analysis in high-grade soft tissue sarcomas. *Genome Biol.* **14**, 137 (2013).

77. Steele, C. D. et al. Undifferentiated Sarcomas develop through distinct evolutionary pathways. *Cancer Cell* **35**, 441–4568 (2019).

78. Sheffield, N. C. et al. DNA methylation heterogeneity defines a disease spectrum in Ewing sarcoma. *Nat. Med.* **23**, 386–395 (2017).

79. Röhrich, M. et al. Methylation-based classification of benign and malignant peripheral nerve sheath tumors. *Acta Neuropathol.* **131**, 877–887 (2016).

80. Wu, S. P. et al. DNA methylation-based classifier for accurate molecular diagnosis of bone Sarcomas. *JCO Precis. Oncol.* **17**, 00031 (2017).

81. Koelsche, C. et al. DNA methylation profiling distinguishes Ewing-like sarcoma with EWSR1-NFATc2 fusion from Ewing sarcoma. *J. Cancer Res. Clin. Oncol.* **145**, 1273–1281 (2019).

82. Miele, E. et al. DNA methylation profiling for diagnosing undifferentiated Sarcoma with Capicua Transcriptional Receptor (CIC) Alterations. *Int. J. Mol. Sci.* **21**, 1818 (2020).

83. Lyskjaer, I. et al. DNA methylation-based profiling of bone and soft tissue tumours: a validation study of the 'DKFZ Sarcoma Classifier'. *J. Pathol. Clin. Res.* **7**, 350–360 (2021).

84. Chakravarty, D. et al. OncoKB: a precision oncology knowledge base. *JCO Precis. Oncol.* **17**, 00011 (2017).

85. Gao, J. et al. Integrative analysis of complex cancer genomics and clinical profiles using the cBioPortal. *Sci. Signal* **6**, 1 (2013).

## ACKNOWLEDGEMENTS

## AUTHOR CONTRIBUTIONS
J.K.D. performed study design, data acquisition, data analysis and interpretation, writing and revision of the paper. F.V., L.H., Y.S., L.Z., S.S., W.T., R.B., T.B., J.B., B.D. performed acquisition, analysis, and/or interpretation of data, and review of the paper. C.R.A. performed study design and conception, analysis and interpretation of data, writing, review and revision of paper. All authors read and approved the final manuscript.

## FUNDING

## COMPETING INTERESTS
The authors declare no competing interests.

## ETHICS APPROVAL AND CONSENT TO PARTICIPATE
This study was approved by the Memorial Sloan Kettering Cancer Institute Institutional Review Board.

## ADDITIONAL INFORMATION
**Supplementary information** The online version contains supplementary material available at https://doi.org/10.1038/s41379-022-01023-9.

**Correspondence** and requests for materials should be addressed to Cristina R. Antonescu.

**Reprints and permission information** is available at http://www.nature.com/reprints

**Publisher's note** Springer Nature remains neutral with regard to jurisdictional claims in published maps and institutional affiliations.